HHS Public Access

Author manuscript

Cell Rep. Author manuscript; available in PMC 2020 September 09.

Published in final edited form as:

Cell Rep. 2020 July 28; 32(4): 107967. doi:10.1016/j.celrep.2020.107967.

Neutrophil Caspase-11 Is Essential to Defend against a Cytosol-Invasive Bacterium

Stephen B. Kovacs[1,2,3,4,6], **Changhoon Oh**[5,6], **Vivien I. Maltez**[3,4], **Benjamin D. McGlaughon**[3,4], **Ambika Verma**[5], **Edward A. Miao**[1,2,3,4,7,*], **Youssef Aachoui**[5,7,8,*]

[1]Department of Immunology, Duke University, Durham, NC 27710, USA

[2]Department of Molecular Genetics and Microbiology, Duke University, Durham, NC 27710, USA

[3]Department of Microbiology and Immunology, Center for Gastrointestinal Biology and Disease, University of North Carolina at Chapel Hill, Chapel Hill, NC 27599, USA

[4]Lineberger Comprehensive Cancer Center, University of North Carolina at Chapel Hill, Chapel Hill, NC 27599, USA

[5]Department of Microbiology and Immunology, Center for Microbial Pathogenesis and Host Responses, University of Arkansas for Medical Sciences, Little Rock, AR 72205, USA

[6]These authors contributed equally

[7]These authors contributed equally

[8]Lead Contact

SUMMARY

Either caspase-1 or caspase-11 can cleave gasdermin D to cause pyroptosis, eliminating intracellular replication niches. We previously showed that macrophages detect *Burkholderia thailandensis* via NLRC4, triggering the release of interleukin (IL)-18 and driving an essential interferon (IFN)-γ response that primes caspase-11. We now identify the IFN-γ-producing cells as a mixture of natural killer (NK) and T cells. Although both caspase-1 and caspase-11 can cleave gasdermin D in macrophages and neutrophils, we find that NLRC4-activated caspase-1 triggers pyroptosis in macrophages, but this pathway does not trigger pyroptosis in neutrophils. In contrast, caspase-11 triggers pyroptosis in both macrophages and neutrophils. This translates to an absolute requirement for caspase-11 in neutrophils during *B. thailandensis* infection in mice. We present an example of inflammasome sensors causing diverging outcomes in different cell types. Thus, cell fates are dictated not simply by the pathogen or inflammasome, but also by how the cell is wired to respond to detection events.

*Correspondence: edward.miao@duke.edu (E.A.M.), yaachoui@uams.edu (Y.A.).

AUTHOR CONTRIBUTIONS

Y.A. and E.A.M. led the project. S.B.K., C.O., Y.A., and E.A.M. wrote the manuscript. C.O., S.B.K., V.I.M., A.V., and Y.A. performed experiments and analyzed results. A.V. and B.D.M. managed the mouse colony.

SUPPLEMENTAL INFORMATION

Supplemental Information can be found online at https://doi.org/10.1016/j.celrep.2020.107967.

DECLARATION OF INTERESTS

The authors declare no competing interests.

Graphical Abstract

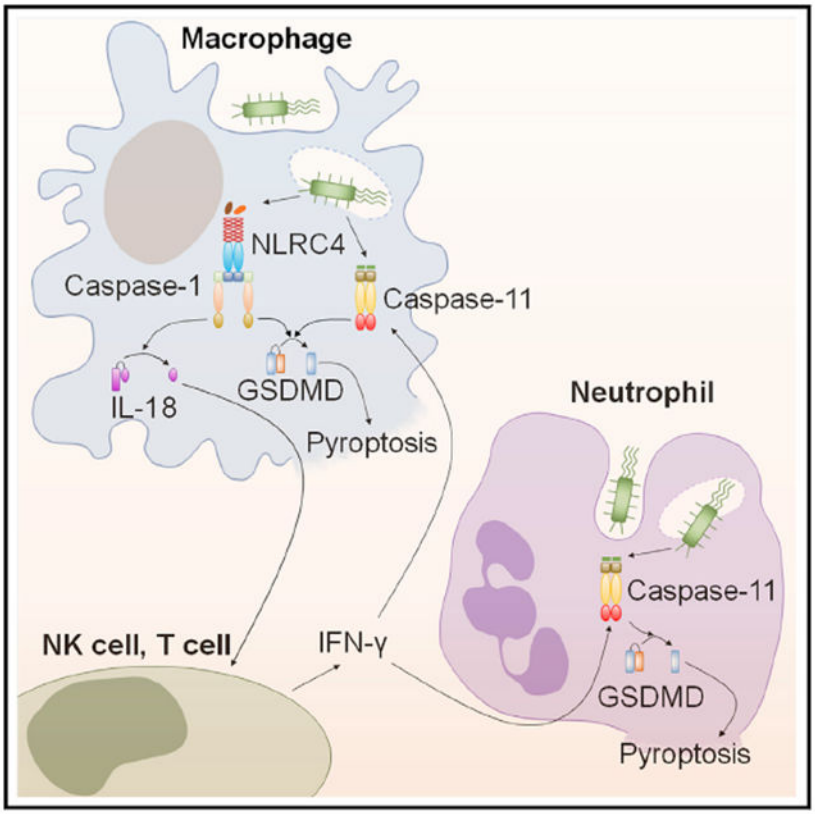

In Brief

Kovacs et al. demonstrate that natural killer and T cells produce IFN-γ to prime caspase-11 during *Burkholderia thailandensis* infection. They demonstrate that in neutrophils, caspase-1 and caspase-11 activation lead to gasdermin D cleavage, but only caspase-11 activation leads to pyroptosis that is necessary for clearance of this cytosol-invasive pathogen *in vivo.*

INTRODUCTION

The innate immune system includes multiple cell types that can be classified as either myeloid cells or lymphocytes that begin acting in defense against pathogens prior to the onset of adaptive responses. The myeloid lineage includes cells like macrophages and neutrophils that function to directly kill bacteria and other pathogens. The innate immune cells with lymphoid lineage include natural killer (NK) cells, innate lymphoid cells (ILCs), and innate-like T cell lymphocytes (Artis and Spits, 2015; Seyda et al., 2016). Networks of cross-talk between myeloid and lymphoid lineages in innate immunity during bacterial infection are a nascent area of study.

Tissue resident macrophages are stationed in all the organs of the body in order to survey for bacterial contamination. They will typically be the first immune cells to come into contact with an infecting bacterium, and thus they are tasked with assessing the threat potential of

the microbe. Cytosolic inflammasome sensors detect the virulence capabilities of pathogens, resulting in the activation of either caspase-1 or caspase-11 (Aachoui et al., 2013b). For example, the NAIP/NLRC4 inflammasome signals to caspase-1 when it detects the activity of virulence-associated bacterial type III secretion systems (T3SS) (Franchi et al., 2006; Miao et al., 2006; 2010b; Molofsky et al., 2006; Ren et al., 2006). This detection alerts the cell to the risk posed: T3SSs inject effector proteins into the host cell cytosol, where these effectors reprogram cellular physiology to benefit the pathogen. In parallel, the caspase-11 inflammasome monitors for lipopoly-saccharide (LPS) contamination as a marker for another virulence trait: cytosolic invasion (Aachoui et al., 2013a; Hagar et al., 2013; Kayagaki et al., 2013). Upon activation, either caspase-1 or caspase-11 can independently cleave and activate the pore-forming protein gasdermin D, triggering lytic cell death called pyroptosis (Kayagaki et al., 2015; Shi et al., 2015). Caspase-1 can also cleave and activate the cytokines interleukin (IL)-1β and IL-18, which are not cleaved by caspase-11 (Ramirez et al., 2018). Typically, *in vitro* studies of pyroptosis have utilized cultured macrophages.

The beneficial responses of caspase-1 and caspase-11 have been studied during infection with many bona fide human pathogens. Interpreting these studies has been complicated by the fact that bona fide pathogens have experienced intense evolutionary pressure to evade inflammasome detection, resulting in inefficient detection by the inflammasome sensors (Maltez and Miao, 2016). On the other hand, many environmental bacteria appear to completely fail to evade inflammasomes, and these are superb model organisms with which to study inflammasome responses (Maltez and Miao, 2016; Maltez et al., 2015). *Burkholderia thailandensis* uses its T3SS to lyse the vacuole and escape into the cytosol, where it replicates (Wiersinga et al., 2006). However, because *B. thailandensis* is not a bona fide mammalian pathogen, it never evolved mechanisms to evade inflammasomes. The result is that wild-type (WT) mice easily identify the extreme virulence capacity of *B. thailandensis* and can eliminate even 20,000,000 colony-forming unit (CFU) systemic challenges within 1 day. In contrast, $Casp1^{-/-}Casp11^{-/-}$ mice succumb to even a 100 CFU challenge (Aachoui et al., 2015). This change in the lethal dose is the strongest inflammasome-dependent defense phenotype of any infectious model as yet published (Maltez and Miao, 2016).

Both NLRC4 and caspase-11 can detect and respond to *B. thailandensis* as well as *Burkholderia pseudomallei*, a related bacterium that causes melioidosis in humans (Aachoui et al., 2013a, 2015; Ceballos-Olvera et al., 2011; Wang et al., 2018). We previously showed that within the first day of infection, the NLRC4 inflammasome is important to limit *B. thailandensis* (Aachoui et al., 2015). Although the resulting caspase-1-driven pyroptosis is probably important, more important was the release of mature IL-18. This IL-18 drove as yet unidentified cells to produce interferon (IFN)-γ, which was critical for priming the caspase-11 inflammasome. Caspase-11 activation then resulted in the clearance of the bacteria, and we previously hypothesized that caspase-11 clearance was mediated via pyroptosis (Aachoui et al., 2015). The importance of NLRC4 and IL-18 could be overcome by persistent infection for 3 days, after which other cytokine responses would also trigger IFN-γ production. However, the importance of IFN-γ and caspase-11 could not be bypassed, because both $Ifng^{-/-}$ and $Casp11^{-/-}$ mice succumbed to the low 100 CFU challenge (Aachoui et al., 2015).

Here, we continue our studies by asking several questions. First, we investigate the cell type(s) that respond to IL-18 by producing IFN-γ, effectively forming a bridge between caspase-1 and caspase-11. Second, we investigate the importance of gasdermin D downstream of caspase-1 and caspase-11. Third, we investigate why the NLRC4-caspase-1 pathway is insufficient to clear *B. thailandensis*, because either caspase-1 or caspase-11 should be competent to drive pyroptosis, and thus they should be functionally redundant.

RESULTS

Multiple Lymphocyte Populations Respond to *B. thailandensis* Infection

We first sought to understand which cell types were responding to the IL-18 by secreting IFN-γ. In the innate immune system, there are two primary cell types that express high levels of the IL-18 receptor (*Il18r1* and *Il18rap*): NK cells and ILCs (Figures S1A and S1B). In the adaptive immune system, activated CD4 and CD8 T cells also express significant levels of the IL-18 receptor.

To assess which cells produce IFN-γ in response to *B. thailandensis* infection, mice were infected with *B. thailandensis* for 12 h, and then treated with brefeldin A (Liu and Whitton, 2005). Splenocytes were collected and assessed for cytokine production by flow cytometric analysis (Figures S2A and S2B). A majority of the cells that produced IFN-γ consisted of $NK1.1^{+}CD3^{-}$ cells, essentially all of which were conventional NK cells ($CD127^{-}$) with only a few ILC1s ($CD90^{+}CD127^{+}$) (Figures 1A–1C and S2C–S2E). A smaller but still substantial population of IFN-γ-producing cells was $CD3^{+}$ T cells (Figures 1A–1C). These $CD3^{+}$ cells consisted of a variety of different T cell subsets (Figures S2F–S2H). While using NK1.1 as opposed to NKp46 to identify NK cells risks underestimating the NK cell population, any underestimation is likely minimal because essentially all IFN-γ-producing $NK1.1^{-}$ cells expressed CD3, which by definition cannot be NK cells.

Interestingly, in the IFN-γ-producing cells, the geometric mean fluorescence intensity (MFI) of IFN-γ was significantly higher in NK cells than T cells (Figures 1D and 1E), suggesting that each NK cell may be producing more IFN-γ than its $CD3^{+}$ counterpart. Remarkably, a median of 36% of the total NK cells in the spleen produced IFN-γ in response to *B. thailandensis* infection (Figure 1F). Together, these data suggest that NK cells and innately responding T cells produce the IFN-γ required to prime caspase-11, and NK cells are exquisitely responsive in this model.

We next asked whether these populations were required to drive the IFN-γ response necessary to clear *B. thailandensis* (Figure 2). First, we examined $Rag1^{-/-}$ mice, which lack all T cells (as well as B cells), but remain competent for NK cells and ILCs. $Rag1^{-/-}$ mice remained fully resistant to *B. thailandensis* infection, surviving both high dose 2×10^{7} and medium dose 10^{4} CFU challenge (Figures 2A and 2E), and sterilizing the burdens in their spleen and liver within 1 day (Figures 2B, 2C, 2F, and 2G). Further, $Rag1^{-/-}$ mice retained their ability to produce significant levels of serum IFN-γ (Figures 2D and 2H), and flow cytometric analysis revealed that, as expected, IFN-γ producing cells were virtually all NK cells (Figure S3A). Therefore, we conclude that NK cells are sufficient to produce IFN-γ to resist *B. thailandensis* infection.

To study mice that genetically lack all these IFN-γ-producing lymphocytes, we used *Rag2*$^{-/-}$ mice that also lack the common γ chain (*Il2rg*), which is required for signaling through several cytokines, including IL-15 that is essential for NK and ILC development (Harly et al., 2018; Robinette et al., 2017). *Rag2*$^{-/-}$*Il2rg*$^{-/-}$ mice were highly susceptible to *B. thailandensis* infection, succumbing to infection and failing to sterilize *B. thailandensis* organ burdens, as was also seen in *Ifng*$^{-/-}$ mice (Figures 2A–2C and 2E–2G). Despite having high bacterial burdens, these mice were defective in their ability to produce IFN-γ (Figures 2D and 2H). The *Rag2*$^{-/-}$*Il2rg*$^{-/-}$ mice and the *Ifng*$^{-/-}$ mice showed equivalent susceptibility during high dose infection, but in the medium dose infection the *Rag2*$^{-/-}$*Il2rg*$^{-/-}$ mice succumbed ~3 days later, and had somewhat lower spleen burdens than seen in *Ifng*$^{-/-}$ mice. This could be due to the fact that *Rag2*$^{-/-}$*Il2rg*$^{-/-}$ mice have altered splenic architecture, which could result in subtle changes in the course of the infection. Alternatively, there may be a very weak source of IFN-γ from non-lymphocytes that slows the infection, but which is not detectable by serum ELISA and ultimately is insufficient to turn the course of the infection.

Finally, we wanted to confirm that the primary role of these cells is to produce IFN-γ, and their cytotoxic function was not involved. Mice deficient in perforin (encoded by *Prf1*), remained fully resistant to *B. thailandensis* infection and had normal levels of serum IFN-γ (Figures S3A and S3B). Furthermore, treatment with exogenous IFN-γ or adoptive transfer of WT NK cells restored resistance to infection in *Rag2*$^{-/-}$*Il2rg*$^{-/-}$ mice, whereas negative controls of PBS or *Ifng*$^{-/-}$ NK cells did not (Figures 2I–2K).

In summary, a variety of lymphocyte populations respond within hours of infection by producing IFN-γ. The predominant responsive cells are NK cells, which are sufficient to produce caspase-11-priming levels of IFN-γ. It is likely that IFN-γ-producing, innately responsive T cells are also sufficient.

Gasdermin D Is Essential for Defense against *B. thailandensis*

We previously showed that pyroptosis of bone marrow-derived macrophages (BMMs) *in vitro* is driven in a redundant manner by both caspase-1 and caspase-11, and only doubly deficient BMMs fully fail to trigger cytotoxicity in response to *B. thailandensis* infection (Aachoui et al., 2013a). Gasdermin D is the recently identified executioner of pyroptosis. In agreement with this, infection of BMMs with *B. thailandensis* triggered gasdermin D cleavage that was dependent on caspase-1 and, to a lesser extent, caspase-11 (Figure 3A). This data would suggest that caspase-1 is more efficient than caspase-11 at cleaving gasdermin D in response to *B. thailandensis,* at least in BMMs. Gasdermin D can be cleaved to activate pore formation by either caspase-1 or caspase-11, and thus one might predict that *Gsdmd*$^{-/-}$ BMMs would resist cytotoxicity and phenocopy *Casp1*$^{-/-}$*Casp11*$^{-/-}$ BMMs. However, this was not the case, because residual LDH release was observed in *Gsdmd*$^{-/-}$ BMMs (Figure 3B). The same was true for IL-1β release as detected by ELISA (Figure 3C). This is actually in agreement with *in vitro* observations by others that found that *Gsdmd*$^{-/-}$ cells still achieve cytotoxicity after inflammasome activation (He et al., 2015; Kayagaki et al., 2015), likely due to apoptotic bypass pathways arising either from a signaling branch point from ASC to caspase-8 (reviewed in Jorgensen et al., 2017) or branching at caspase-1

itself to BID (Tsuchiya et al., 2019), followed by secondary necrosis. While the ASC to caspase-8 pathway should still be functional in *Casp1*$^{-/-}$*Casp11*$^{-/-}$ mice, the caspase-1 to BID pathway may be faster, which could explain why *Gsdmd*$^{-/-}$ BMMs have higher levels of cytotoxicity at this time point compared to *Casp1*$^{-/-}$*Casp11*$^{-/-}$ BMMs. These data would suggest that loss of gasdermin D during infection *in vivo* could be less impactful than the combined effect of the loss of caspase-1 and -11.

We next examined the role of gasdermin D in defense against *B. thailandensis in vivo.* We previously showed that the *Casp1*$^{-/-}$ proxy mice, *Nlrc4*$^{-/-}$*Asc*$^{-/-}$, succumb only to high dose 2×10^7 CFU infection by *B. thailandensis*, and survive medium 10^4 CFU challenges (Aachoui et al., 2015). We now verify that this also holds true in the clean single knockout *Casp1*$^{-/-}$ mice, whereas *Casp11*$^{-/-}$ mice were verified again to succumb (Figures 4A and 4B). Although caspase-1 plays a lesser role, it can also be seen to slow the course of infection; thus, the caspase-1-sufficient *Casp11*$^{-/-}$ mice succumb slower than *Casp1*$^{-/-}$*Casp11*$^{-/-}$ mice (Aachoui et al., 2015) (replicated in Figures 4A and 4B). This is the opposite of the *in vitro* data where caspase-1 appeared to be more efficient in cleaving gasdermin D (in BMMs).

Gsdmd$^{-/-}$ mice succumbed to the high 2×10^7, medium 10^4, and low 10^2 CFU dose challenges, with kinetics that matched *Casp1*$^{-/-}$*Casp11*$^{-/-}$ mice but were faster than *Casp11*$^{-/-}$ mice (Figures 4A–4C). We further quantitated these results by determining bacterial burdens at day 1 after high dose challenge, or at day 2 following medium dose challenge. *Gsdmd*$^{-/-}$ mice had the highest burdens on par with *Casp1*$^{-/-}$*Casp11*$^{-/-}$ mice, with *Casp11*$^{-/-}$ only slightly lower, and *Casp1*$^{-/-}$ or their proxy *Nlrc4*$^{-/-}$*Asc*$^{-/-}$ mice having lower burdens still, and WT mice clearing both doses (Figures 4D–4G). Together, these results indicate that bypass pathways to other forms of cell death cannot compensate for the loss of pyroptosis in *Casp1*$^{-/-}$*Casp11*$^{-/-}$ mice or in *Gsdmd*$^{-/-}$ mice. This is also in agreement with Wang et al. (2019) who observed that *Gsdmd*$^{-/-}$ and *Casp1*$^{-/-}$*Casp11*$^{-/-}$ mice were more susceptible than WT mice to intranasal infection with *B. thailandensis*.

We previously showed that the importance of NLRC4-ASC and caspase-1 is seen only in the first 3 days of infection when they drive IL-18 release, which in turn triggers IFN-γ production (Aachoui et al., 2015). We now asked whether gasdermin D was important for this release of IL-18. As expected, IL-18 release within the first day of infection was dependent on gasdermin D (Figures 4H and 4I). Casp1$^{-/-}$Casp11$^{-/-}$ control mice with equivalent burdens to *Gsdmd*$^{-/-}$ mice also did not have detectable levels of serum IL-18 (Figures 4H and 4I).

Interestingly, at a later time point, day 2 post-infection, we observed elevated serum IL-18 in *Gsdmd*$^{-/-}$ mice, and a trending elevation in *Casp1*$^{-/-}$*Casp11*$^{-/-}$ mice that did not reach statistical significance (Figures 4J and 4K). Notably, the ELISA kit we used to measure the IL-18 levels was specific for the cleaved, active form of IL-18 (Figure S4). Our data are consistent with that of Wang et al. (2019), who observed a delayed elevation of IL-18 levels in bronchoalveolar lavage fluid from *Gsdmd*$^{-/-}$ mice infected intranasally with *B. thailandensis.* In *Gsdmd*$^{-/-}$ mice, the IL-18 is likely still cleaved by caspase-1 and is released in a delayed manner after non-pyroptotic necrosis of the cell, perhaps secondary to

the backup pathways that have been observed *in vitro*. Alternatively, this serum IL-18 may arise from non-specific tissue damage caused by sepsis that activates caspase-1 in uninfected cells, because these mice had exceptionally high, near-lethal bacterial burdens (Figure 4J). Indeed, these mice are expected to succumb to the infection by the end of the day of harvest in this experiment (Figure 4B). How IL-18 is cleaved in *Casp1*$^{-/-}$*Casp11*$^{-/-}$ mice, however, is harder to explain. One possibility is that the ASC backup pathway-mediated caspase-8 activation results in caspase-8 cleaving IL-18 (Bossaller etal., 2012). Indeed, consistent with this backup pathway having a subtle effect, we observed that *Casp1*$^{-/-}$ mice (in which the ASC-caspase-8 backup pathway remains intact) survived a day longer to high dose challenge and had a small but statistically significant reduction in burdens when compared to *Nlrc4*$^{-/-}$*Asc*$^{-/-}$ mice (in which this backup pathway is deficient) (Figures 4A, 4D, and 4F). Alternatively, unprocessed IL-18 may be released by non-pyroptotic necrosis, and IL-18 could then be cleaved extracellularly. Indeed, several extracellular proteases have been reported as capable of cleaving and activating IL-18, including chymase and granzyme B (Afonina et al., 2015). Regardless of the mechanism, we can conclude that the delayed release of IL-18 is inadequate to clear infection in *Gsdmd*$^{-/-}$ and *Casp1*$^{-/-}$*Casp11*$^{-/-}$ mice.

Caspase-11, but Not Caspase-1, Triggers Pyroptosis in Neutrophils

Next, we considered the apparent paradoxical separation of the phenotypes of *Casp1*$^{-/-}$ and *Casp11*$^{-/-}$ mice. Because both caspase-1 and caspase-11 should be competent to cleave gasdermin D independently of each other, one would expect redundancy in which *Casp1*$^{-/-}$*Casp11*$^{-/-}$ mice and *Gsdmd*$^{-/-}$ mice would be equally susceptible, whereas single *Casp1*$^{-/-}$ and *Casp11*$^{-/-}$ mice both remain resistant to infection. However, this was not the case, because caspase-1 could not substitute for caspase-11 in defense (Aachoui et al., 2015; Wang et al., 2018).

In considering why NLRC4 and caspase-1 were not sufficient to clear *B. thailandensis,* we hypothesized that there was a cell type *in vivo* that failed to activate NLRC4, and thus a single *Casp11*$^{-/-}$ mouse would phenocopy the double knockout in that cell type. One potential candidate cell type is the neutrophil. WT mice have been shown to effectively kill *Salmonella enterica* serovar Typhimurium when engineered to overexpress the NLRC4-agonist flagellin (Miao et al., 2010a). However, if neutrophils are unable to kill phagocytosed bacteria due to loss of the ability to produce reactive oxygen species (*Ncf1*$^{-/-}$ mice lacking the phagocyte oxidase), then flagellin-engineered *S.* Typhimurium will persist and replicate inside a vacuole within neutrophils (Miao et al., 2010a). This observation suggests that neutrophils do not effectively undergo pyroptosis when exposed to NLRC4 agonists. Consistent with this concept, Chen et al. (2014, 2018) showed that treatment of neutrophils with NLRC4 agonists triggers caspase-1 activation to promote IL-1β maturation but does not result in pyroptosis. In contrast, neutrophil exposure to cytosolic LPS drives caspase-11 activation and gasdermin D cleavage to induce pyroptosis (Chen et al., 2018). We thus hypothesized that neutrophils were anergic to NLRC4, but would undergo pyroptosis in response to caspase-11 activation during *B. thailandensis* infection.

First, we wanted to compare macrophage and neutrophil responsiveness to NLRC4 and caspase-11 agonists. To activate NLRC4, we treated BMMs and bone marrow neutrophils

with the well characterized NLRC4 agonist PrgJ-Tox (Zhao et al., 2011). To activate caspase-11, we transfected LPS into the cytoplasm of the cells. Treatment with PrgJ-Tox and cytoplasmic LPS resulted in gasdermin D cleavage in both macrophages and neutrophils, showing that both NLRC4 and caspase-11 activation produce active gasdermin D (Figures 5A and 5B). Caspase-11 activation with cytoplasmic LPS induced caspase-11-dependent cell death as well as IL-1β release in both macrophages and neutrophils (Figures 5C, 5D, 5G, and 5H). It is worth noting that although we did not observe significant cleavage of caspase-11 by western blot, we have historically found western blots to be an unreliable way to evaluate caspase-11 activation compared to the downstream effects of caspase-11 activation like pyroptosis or gasdermin D cleavage (Hagar et al., 2013). In contrast to caspase-11 activation, although NLRC4 activation with PrgJ-Tox induced release of IL-1β from both macrophages and neutrophils, NLRC4 activation induced significant levels of cell death in macrophages, but not in neutrophils (Figures 5E, 5F, 5I, and 5J).

We next wanted to evaluate inflammasome responses of neutrophils to *B. thailandensis* infection *in vitro*. We infected neutrophils from WT, *Casp1*$^{-/-}$, and *Casp11*$^{-/-}$ mice with *B. thailandensis*. Consistent with our data with PrgJ-Tox and cytoplasmic LPS, WT, *Casp1*$^{-/-}$, and *Casp11*$^{-/-}$ neutrophils all exhibited comparable levels of gasdermin D cleavage, demonstrating that caspase-1 and caspase-11 are both sufficient to activate gasdermin D in response to *B. thailandensis* (Figure 6A). As expected, release of IL-1β depended on caspase-1, but not caspase-11 (Figure 6B), consistent with NLRC4 being sufficient to drive caspase-1 activation. However, neutrophil cytotoxicity in response to *B. thailandensis* depended only on caspase-11 (Figure 6C), suggesting that NLRC4 activation of caspase-1 is insufficient to cause pyroptosis. This is the opposite of what we observed in macrophages, where caspase-1 was more efficient at causing gasdermin D cleavage and cell death in response to *B. thailandensis* (Figures 1A and 1B). These data agree with data from Chen et al. (2014, 2018) showing that NLRC4 activation triggers cytokine release but not pyroptosis in neutrophils. However, unlike Chen et al. (2018), who found that caspase-1 inefficiently cleaved gasdermin D in neutrophils, we found that caspase-1 was similarly efficient as caspase-11 at cleaving gasdermin D in neutrophils, although we agree with Chen et al. (2018) that this did not result in pyroptosis. This difference is likely attributable to PrgJ-Tox and *B. thailandensis* being more efficient at delivering the NLRC4 agonists into the cytosol than transfection of flagellin using FuGene as performed by Chen et al., 2018. The mechanism whereby neutrophils survive the gasdermin D activation downstream of caspase-1, but not caspase-11, remains to be elucidated.

Finally, to assess the effect of inflammasome activation on the ability for neutrophils to harbor *B. thailandensis,* we infected neutrophils *in vitro* with *B. thailandensis* and examined bacterial recovery in the presence of extracellular membrane-impermeant kanamycin, which kills extracellular bacteria as well as those trapped in pyroptotic cells with ruptured membranes. No bacteria were recovered from WT or *Casp1*$^{-/-}$ neutrophils, whereas *Casp11*$^{-/-}$ neutrophils had significant bacterial recovery (Figure 6D). This indicates that *B. thailandensis* can survive within *Casp11*$^{-/-}$ neutrophils *in vitro*. This also suggests that the proposed direct bactericidal activity of cleaved gasdermin D (Liu et al., 2016; Wang et al., 2019), which forms robustly downstream of caspase-1 in these cells (Figure 5), is insufficient to clear *B. thailandensis*, consistent with our *in vivo* data indicating that

caspase-1 alone cannot clear *B. thailandensis* infection (Figures 4B and 4F comparing *Casp1*$^{-/-}$ to *Casp11*$^{-/-}$ mice).

Neutrophil Caspase-11 Is Essential for Survival of Mice Infected with *B. thailandensis*

Next, we examined the importance of neutrophil caspase-11 during *B. thailandensis* infection *in vivo.* To delete caspase-11 primarily in neutrophils while retaining it in most other cells, we crossed *Casp1*$^{fl/fl}$ mice with *Mrp8* promoter-driven *cre* transgene mice. *Mrp8-cre* deletes model floxed genes at 80% efficiency in splenic, peripheral blood, and bone marrow neutrophils, while deleting at 0%–20% efficiency in monocyte and macrophage populations (Abram et al., 2014). Thus, *Mrp8-cre* has been used for neutrophil-specific deletions. In contrast, *LysM-cre* deletes in both macrophages and neutrophils (Abram et al., 2014). Both *Casp11*$^{fl/fl}$*Mrp8-cre* and *Casp11*$^{fl/fl}$*LysM-cre* mice were highly susceptible to *B. thailandensis* infection, showing bacterial burdens and survival kinetics that approached that of full body knockout controls (Figures 7A–7C). This suggests that caspase-11 is absolutely essential in the neutrophil compartment.

The caveat to drawing definitive conclusions from the use of *Mrp8-cre* mice is that this *cre* line also causes a relatively smaller 0%–20% deletion in monocytes and macrophages (Abram et al., 2014). To determine if a potential deletion of caspase-11 in 20% of macrophages could account for the phenotypes observed in *Casp11*$^{fl/fl}$*Mrp8-cre* mice, we created mixed bone marrow chimeras with a ratio of 20% of *Casp11*$^{-/-}$: 80% WT bone marrow marked with CD45.2^{+} and CD45.1^{+}, respectively. Maintenance of this ratio upon engraftment was verified by flow cytometry (Figure S5). In these mice, 20% of both macrophages and neutrophils are completely deficient in caspase-11 and therefore could serve as intracellular niches for *B. thailandensis*. Notably, after infection with *B. thailandensis*, bacterial burdens in these mice were comparable to those of control mice engrafted with 1% *Casp1*$^{-/-}$ 99% WT bone marrow, and significantly lower than mice engrafted with 99% *Casp11*$^{-/-}$: 1 % WT bone marrow (Figures 7D and 7E). Thus, having 20% *Casp11*$^{-/-}$ monocytes and macrophages does not cause susceptibility to *B. thailandensis* infection, arguing that the phenotype of the *Mrp8-cre* mice cannot be attributed to deletion in the monocyte/macrophage compartments. We can also conclude that having 20% *Casp11*$^{-/-}$neutrophils was not sufficient to cause susceptibility, suggesting that the immune system can overcome a relatively small fraction of susceptible cells that harbor the infection. In summary, deletion of *Casp11* in *Mrp8-cre* marked cells, most of which are neutrophils, is sufficient to cause susceptibility to *B. thailandensis* infection. However, we do not exclude the possibility that deletion of *Casp11* in other cell types could also be sufficient to cause susceptibility.

Gasdermin D in neutrophils has recently been suggested to cause the formation of neutrophil extracellular traps (NETs) (Chen et al., 2018; Sollberger et al., 2018). Typically, NET formation is dependent upon the activity of both the NADPH oxidase (that includes p47^{phox} encoded by *Ncf1*) and neutrophil elastase (encoded by *Elane*), and in some cases myeloperoxidase (MPO). We therefore infected *Elane*$^{-/-}$, *Ncf1*$^{-/-}$, and *Mpo*$^{-/-}$ mice with *B. thailandensis. Elane*$^{-/-}$ mice remained fully resistant, whereas *Ncf1*$^{-/-}$ mice had lower bacterial burdens than *Casp11*$^{-/-}$ mice at both medium and high doses (Figures 7F and 7G).

The *Ncf1*$^{-/-}$ results are in agreement with our previous observation that *Ncf1*$^{-/-}$ mice succumbed to *B. thailandensis* infection significantly slower than *Casp1*$^{-/-}$*Casp11*$^{-/-}$ mice (*Ncf1*$^{-/-}$ mice succumb between days 6–11, whereas *Casp1*$^{-/-}$*Casp11*$^{-/-}$ mice succumb at day 2 to a 10^4 CFU challenge) (Maltez and Miao, 2016). The phenotype in *Ncf1*$^{-/-}$ mice could be due to the role of p47^{phox} in direct bactericidal activity via reactive oxygen species, or to its role in NETosis. Finally, *Mpo*$^{-/-}$ mice remained fully resistant to infection (Figure 7H). Thus, the genes that are traditionally required for NET formation have weaker phenotypes than caspase-11.

DISCUSSION

We identify a coordinated innate immune defense pathway whereby initial detection of *B. thailandensis* by the NLRC4 inflammasome activates caspase-1, resulting in IL-18 release, and also likely a modestly beneficial pyroptosis. These responses occur quickly, but alone are unable to clear the infection. Next, a variety of lymphocytes, primarily NK cells and T cells, respond to the IL-18 by secreting IFN-γ, which is essential for defense. IFN-γ is required to prime caspase-11. Among caspase-11-responding cells, activation of caspase-11 in neutrophils is absolutely essential for defense. Caspase-11 activates the pyroptotic pore gasdermin D, which kills the infected neutrophil and removes an important intracellular niche for *B. thailandensis*.

We demonstrate that NK cells are the largest population that produces IFN-γ in this model. However, T cells also respond innately and produce IFN-γ. This T cell population is a conglomeration of various T cells subset, likely including both innate T cells like gamma delta T cells and NK T cells, as well as possibly conventional T cells responsive to IL-18 (Kupz et al., 2012). Although ILC1s were not a major producer of IFN-γ in this model likely owing to their small population in the spleen, it would be interesting to determine if resident ILC1s play a major role in other tissues where resident ILC1s are more prevalent.

Why is the immune system organized in such a way that caspase-1 must respond first, then lymphocytes must assess the total caspase-1 response via monitoring for IL-18, and only then will the resulting IFN-γ prime caspase-11? We propose that because caspase-11 detects LPS, a ubiquitous component of both commensal and pathogenic gram-negative bacteria, it is more prone to false-positive responses than NLRC4, which more directly detects virulence in the form of T3SS activity. False-positives can result in aberrant pyroptosis that is damaging to tissues and can lead to sepsis (Hagar et al., 2013, 2017; Kayagaki et al., 2013). Therefore, caspase-11 is placed behind a priming firewall designed to only be opened only when the immune system has reason to “believe” that it is likely that a cytosol-invasive pathogen is present. This likelihood arises from detection of T3SS activity in the case of *B. thailandensis*, and the judgement is made by NK cells and T cells.

Most work on inflammasomes has been done in macrophages. Indeed, despite the fact that neutrophils are quickly recruited in copious numbers to sites of early infection, it is unclear to what extent inflammasomes are activated in neutrophils or what role this activation could play in neutrophil function. We have now bridged that gap by characterizing the importance of the neutrophil caspase-11 inflammasome *in vitro* and *in vivo*. We show that NLRC4

activation fails to clear bacteria from neutrophils, whereas caspase-11 accomplishes this task with extreme efficiency. This leads us to ask: what is the benefit of having neutrophils not respond to NLRC4 agonists with pyroptosis, and why would that be different with caspase-11? Furthermore, why would neutrophils use these inflammasomes in different ways compared to macrophages?

As tissue-resident sentinel cells, macrophages are the first responders to infection. Macrophages monitor for the activity of T3SS, and trigger pyroptosis to convert an infected cell into a pore-induced intracellular trap (PIT). We previously showed that this process does not kill the bacteria, but instead detains them within the remains of the pyroptotic macrophage while simultaneously elaborating neutrophil chemoattractants. Neutrophils then efferocytose the PIT and the bacteria contained inside and kill the bacteria through the activity of potent microbicidal effectors like NADPH oxidase (Jorgensen et al., 2016). In this way, macrophages have the luxury of “passing the buck” to the neutrophil, a more bactericidal cell type.

Neutrophils, however, may not have the luxury of passing a bacterium to another cell. Perhaps, in most cases, they do not need to do so. If a neutrophil encountered a T3SS-positive bacterium, it should expect that it will phagocytose and kill the bacterium. If the neutrophil were instead to kill itself, the neutrophil might fail to kill the bacterium, especially if the bacterium was still extracellular. Thus, neutrophils might be best suited to continue to live and to fight against infection as long as the bacterium remains in the vacuole, which is the primary location for neutrophil bactericidal mechanisms. On the other hand, caspase-1-driven cytokine release would be beneficial, because a T3SS positive bacterium has a higher threat level and warrants recruitment of a greater inflammatory response.

In contrast, what would happen to a neutrophil if bacteria escape into the cytosol? *B. thailandensis* escapes to the cytosol of most cells within 15 min (Wiersinga et al., 2006). Because most bactericidal activity of the neutrophil is directed at the vacuole, the event of cytosolic invasion may represent complete evasion of the neutrophil’s primary function. Hence, caspase-11-driven pyroptosis should be critical to deny cytosol-invasive bacteria a niche within neutrophils.

One major outstanding question is if NLRC4 and caspase-1 activation are sufficient to produce significant levels of cleaved gasdermin D in neutrophils, why do neutrophils not undergo pyroptosis after caspase-1 activation? Chen et al. (2018) suggested that caspase-1 was unable to cleave sufficient amounts of gasdermin D in the neutrophil. In contrast, we used more efficient means of NLRC4 agonist delivery, and we now observed robust caspase-1-dependent gasdermin D cleavage, but this still failed to cause pyroptosis. The mechanism is likely explained by a recent publication, in which Karmakar et al. (2020) observed that NLRP3-driven caspase-1 activation did not result in significant accumulation of gasdermin D on the neutrophil plasma membrane, but instead gasdermin D accumulated on the membrane of azurophilic granules. Likely, the large number of granules packed in each neutrophil could serve as a membrane sink for gasdermin D. During caspase-1 activation, the ASC speck usually forms perinuclearly (Fernandes-Alnemri et al., 2007;

Sahillioglu et al., 2014). Thus, gasdermin D cleaved at the ASC speck must diffuse from the perinuclear location to the outer membrane, and it would likely encounter and insert into granule membranes instead. One idea that is raised by gasdermin D pores inserting into neutrophil granules is the possibility that this could release granule bactericidal components to the cytosol, thereby killing cytosol-invasive bacteria (Karmakar et al., 2020). However, in the case of *B. thailandensis*, our data show that this hypothetical mechanism is insufficient because caspase-1-sufficient *Casp11*$^{-/-}$ still succumb to infection.

In contrast to caspase-1, Chen et al. (2018) and our data indicate that caspase-11 activation is sufficient to cause pyroptosis. Karmakar et al. (2020) did not study the localization of gasdermin D after caspase-11 activation; however, their model introduces concepts that may explain the difference. We speculate that caspase-11 can be activated more diffusely throughout the cell. This diffuse caspase-11 could cleave gasdermin D in closer proximity to the plasma membrane. The resulting plasma membrane pores would be more likely to cause neutrophil pyroptosis. This hypothesis will be explored in future work.

In summary, our work describes how a single pathogen, *B. thailandensis*, can be detected by apparently redundant inflammasome pathways. However, these pathways are deployed differentially in macrophages compared to neutrophils. This must be driven by the different cellular characteristics and immunologic functions of the macrophage as compared to the neutrophil. This study illustrates the importance of studying inflammasomes *in vivo* where complex cellular interactions occur.

STAR★METHODS

RESOURCE AVAILABILITY

Lead Contact—Further information and requests for resources and reagents should be directed to and will be fulfilled by the Lead Contact, Dr. Youssef Aachoui (YAachoui@uams.edu).

Materials Availability—Mouse lines generated for this paper are available by request to the lead contact.

Data and Code Availability—Source data for Figure S1 is available through the Immunological Genome Project (http://rstats.immgen.org/Skyline_microarray/skyline.html) and can be accessed by searching through the microarray database for IL18R (probe set ID 10345807) and IL18RAP (probe set ID 10345824).

EXPERIMENTAL MODEL AND SUBJECT DETAILS

Mice—Wild-type (WT) C57BL/6 (Jackson Laboratory), *Casp1*$^{-/-}$ (Rauch et al., 2017), *Nlrc4*$^{-/-}$*Asc*$^{-/-}$ (Aachoui et al., 2015), *Casp*$^{-/-}$ (Kayagaki et al., 2011), *Casp1*$^{-/-}$*Casp11*$^{129mut/129mut}$ referred to as *Casp1*$^{-/-}$*Casp11*$^{-/-}$ (Kuida et al., 1995), *Elane*$^{-/-}$ (Jackson # 006112), *Mpo*$^{-/-}$ (Jackson Laboratory # 004265), *Ncf1*$^{mt/mt}$ referred to as *Ncf1*$^{-/-}$ (Jackson # 004742), *Prf1*$^{-/-}$ (Jackson # 002407), *Rag1*$^{-/-}$ (Jackson # 002216), *Rag2*$^{-/-}$*Il2rg*$^{-/-}$ (Taconic # 4111), *Gsdmd*$^{-/-}$ (Rauch et al., 2017), *Ifng*$^{-/-}$ (Jackson # 002287), *Casp11*$^{fl/fl}$ (Cheng et al., 2017), *Mrp8-cre* (Jackson # 021614), and *LysM-cre*

(Jackson # 004781) mice were used in this study. All mice were 6-12 weeks old, male or female, and housed under specific pathogen free condition-free facilities. All protocols were approved by the Institutional Animal Care and Use Committee at the University of Arkansas for medical Sciences at Little Rock, or Institutional Animal Care and Use Committee at the University of North Carolina at Chapel Hill.

Bacterial strains—In this study, we used a *Burkholderia thailandensis* strain that we previously passaged through *Casp1*$^{-/-}$*Casp11*$^{-/-}$ mice (*B. thailandensis*, strain E264-1); this strain displays more synchronized infection kinetics than the parental E264 (Aachoui et al., 2015).

Primary cells—Primary neutrophils were isolated from mouse bone marrow using Neutrophil Isolation Kit (Miltenyi Biotec) using manufacturer instruction.

Bone marrow-derived macrophages (BMM) were prepared from the femur and tibia of mice by culturing with L929 cell supernatant for 7 day at 37°C, 5% CO_2.

METHOD DETAILS

***In vivo* infections—**For all experiments, *Burkholderia thailandesis* were grown in Luria-Bertani medium (LB) overnight at 37°C. Bacteria were pelleted from 1 mL of culture and washed in PBS before inoculation to mice. Bacteria titer was determined by OD measurement at 600 nm and plating serial dilution on LB agar plates. For lethal challenge, mice were inoculated via the intraperitoneal (i.p.) route with the doses specified in the text. For bacterial burden measurements, spleens and livers were collected on day 1 when dose of infection used 2x10^7 CFU, and on day 1 or 2 post-infection when dose of infection used was 10^4 CFU. All organ harvested were homogenized in sterile PBS. Viable CFUs in homogenates were enumerated by plating serial dilutions on agar plates. At the same time of organ harvest, serum was collected from blood drawn by cardiac puncture for cytokines measurement. ELISA assays were performed per manufacturer instructions to measure serum levels of mouse IL-18 (MBL International) and IFN-γ (R&D Systems). Alternatively, in Figure 2I, *Rag1*$^{-/-}$, *Rag2*$^{-/-}$*Il2rg*$^{-/-}$ or *Ifng*$^{-/-}$ mice were infected i.p. with 2x10^6 CFU of *B. thailandensis*, and treated with recombinant murine IFN-γ (0.5 mg/mice) at the time of infection and 24 h post-infection. Bacterial burdens in organ homogenates were determined as described above. In Figures 2J and 2K, *Rag1*$^{-/-}$*Il2rg*$^{-/-}$ mice were adoptively treated (tail vain injection) at day −14 and −7 with 10^6 cells of IL-2-expanded WT or *Ifng*$^{-/-}$ NK cells. Fourteen days after first adoptive transfer, mice were infected i.p. with 10^{4}CFU of *B. thailandensis*. Bacterial burdens in organ homogenates were determined 72 h post-infection as described above.

***In vitro* infection and analysis of inflammasome activation—**For *in vitro* infections, *B. thailandensis* grown as described above were pelleted from 1 mL of culture were opsonized with 50 μL of mouse sera for 30 min at 37°C and then suspended in 1 mL of DMEM. BMMs were prepared as described (Miao et al., 2010a). For infections, macrophages were seeded into 96-well tissue culture treated plates at a density of 5x10^4 cells/well. Macrophages were primed with Pam_3CSK_4 (1 μg/ml) (InvivoGen) overnight.

Bacteria were added to BMMs at MOI 50, centrifuged for 5 min at 300 g, and then incubated at 37°C for 1hr. After 1 h, extracellular bacterial growth was stopped by addition of 300 μg/ml kanamycin and supernatant samples were collected at 3 h. For neutrophil infections, bone marrow neutrophils (isolated using Neutrophil Isolation Kit (Miltenyi Biotec)) were seeded into 96-well tissue culture treated plates at a density of $4x10^5$ cells/well. Neutrophil were primed with Pam_3CSK_4 (1 μg/ml) (InvivoGen) for 4 h. Bacteria were added to BMMs at MOI 100, centrifuged for 5 min at 300 g, and then incubated at 37°C for 1 h. After 1 h, extracellular bacterial growth was stopped by addition of 300 μg/ml kanamycin, and CFU was determined at 5 h. Alternatively, macrophages or neutrophils were primed with IFN-γ (10 ng/ml, Peprotech) and ultra-pure LPS (50 ng/ml) (*E. coli* O111:B4; InvivoGen) for 4 hours. Then, cells were treated with NLRC4 agonist PrgJ-Tox (Zhao et al., 2011) (2 μg/ml) or transfected with LPS (10 μg/ml) for 5 h. Cytotoxicity was defined as the percentage of total lactate dehydrogenase released into the supernatant and was determined as described (Rayamajhi et al., 2013). IL-1β secretion was determined by enzyme-linked immunosorbent assay (ELISA) (R&D Systems). Lysates and supernatants were combined and analyzed by western blot for GSDMD activation (EPR19828; Abcam), caspase-1 activation (Casper-1; AdipoGen), caspase-11 (EPR18628; Abcam) and actin (ACTN05 (C4); Invitrogen)

IFN-γ intracellular cytokine staining—WT C57BL/6 or *Rag1*$^{-/-}$ mice were infected with $2x10^7$ CFU of *B. thailandensis*. Twelve h later, mice were i.v. treated with 250 μg, i.v of brefeldin A (Sigma-Aldrich) as previously described (Liu and Whitton, 2005). 6 h later, mice were euthanized, spleens were harvested, and splenocytes were extracted by mechanical disruption. Red blood cells were lysed with ACK lysing buffer, and splenocytes were counted using a hemocytometer. $2x10^6$ cells from each spleen were first stained with LIVE/DEAD Fixable Blue Dead Cell Stain Kit (Thermo Fisher) followed by extracellular staining for 30 min at room temperature. Extracellular antibodies used include: Alexa Fluor (AF) 488 anti-CD127 (clone A7R34); Brilliant Violet (BV) 570 anti-CD3 (clone 17A2); APC-Cy7 anti-CD45R (clone RA3-6B2); APC-Cy7 anti-Ly6G (clone 1A8); PE-Cy7 anti-CD90.2 (clone 53-2.1); BV650 anti-NK1.1 (clone PK136); BV421 anti-TCR γδ (clone GL3). For analyzing the distribution of CD4 and CD8 T cells, a parallel aliquot of cells was stained using the same panel as above with AF594 anti-CD4 (clone GK1.5) and PE anti-CD8 (clone 53-6.7). Cells were then fixed and permeabilized with BD Cytofix/Cytoperm for 20 min at 4°C before being stained with APC anti-IFN-γ (clone XMG1.2; BioLegend). Cells were washed, acquired on a BD LRSII (UNC Flow Cytometry Core Facility), and analyzed using FlowJo (TreeStar; version 9.9.6). All antibodies were purchased from BioLegend. Absolute counts were determined by multiplying frequencies of population of interest determined by flow cytometry with the total number of splenocytes collected as determined by hemocytometer.

QUANTIFICATION AND STATISTICAL ANALYSIS

All statistics were performed using Prism 8 (GraphPad) using either two-way ANOVA followed by Sidak's multiple comparison test, one way ANOVA followed by Tukey's multiple comparison test, or Log-rank as specified in the figure legends. Number of mice

used in each *in vivo* survival experiment are specified in Table S1. Flow data were analyzed using FlowJo (TreeStar; version 9.9.6).

Supplementary Material

Refer to Web version on PubMed Central for supplementary material.

ACKNOWLEDGMENTS

We wish to thank Vishva Dixit, Nobuhiko Kayagaki, Richard Flavell, and Russell Vance for sharing mice. We also thank Farhan Lakhani, Maria (Maca) Artunduaga, and Taylor Abele for upkeep of our mouse colony and Charles Kroger for assisting with some of the experiments. This work was supported by grants from the National Institutes of Health (NIH) (AI097518, AI133236, AI139304, AI119073, and AI136920 to E.A.M, 1K22AI132489-01 to Y.A., and F30AI142990 to S.B.K.), and a grant from the NIH with the National Institute of General Medical Sciences (NIGMS) (P20-GM103625 to Y.A). E.A.M. is supported by the Yang Biomedical Scholars Award. The University of North Carolina (UNC) Flow Cytometry Core Facility is supported in part by a National Cancer Institute (NCI) Center Core Support Grant (P30CA016086) to the UNC Lineberger Comprehensive Cancer Center. We also acknowledge the University of Arkansas for Medical Sciences (UAMS) Center for Microbial Pathogenesis and Host Inflammatory Responses (CMPHIR) for continued support and the UAMS Flow Cytometry Core Facility for technical assistance.

REFERENCES

Aachoui Y, Leaf IA, Hagar JA, Fontana MF, Campos CG, Zak DE, Tan MH, Cotter PA, Vance RE, Aderem A, and Miao EA (2013a). Caspase-11 protects against bacteria that escape the vacuole. Science 339, 975–978. [PubMed: 23348507]

Aachoui Y, Sagulenko V, Miao EA, and Stacey KJ (2013b). Inflammasome-mediated pyroptotic and apoptotic cell death, and defense against infection. Curr. Opin. Microbiol. 16, 319–326. [PubMed: 23707339]

Aachoui Y, Kajiwara Y, Leaf IA, Mao D, Ting JP-Y, Coers J, Aderem A, Buxbaum JD, and Miao EA (2015). Canonical Inflammasomes Drive IFN-γ to Prime Caspase-11 in Defense against a Cytosol-Invasive Bacterium. Cell Host Microbe 18, 320–332. [PubMed: 26320999]

Abram CL, Roberge GL, Hu Y, and Lowell CA (2014). Comparative analysis of the efficiency and specificity of myeloid-Cre deleting strains using ROSA-EYFP reporter mice. J. Immunol. Methods 408, 89–100. [PubMed: 24857755]

Afonina IS, Müller C, Martin SJ, and Beyaert R (2015). Proteolytic Processing of Interleukin-1 Family Cytokines: Variations on a Common Theme. Immunity 42, 991–1004. [PubMed: 26084020]

Artis D, and Spits H (2015). The biology of innate lymphoid cells. Nature 517, 293–301. [PubMed: 25592534]

Bossaller L, Chiang P-I, Schmidt-Lauber C, Ganesan S, Kaiser WJ, Rathinam VAK, Mocarski ES, Subramanian D, Green DR, Silverman N, et al. (2012). Cutting edge: FAS (CD95) mediates noncanonical IL-1β and IL-18 maturation via caspase-8 in an RIP3-independent manner. J. Immunol. 189, 5508–5512. [PubMed: 23144495]

Ceballos-Olvera I, Sahoo M, Miller MA, Del Barrio L, and Re F (2011). Inflammasome-dependent pyroptosis and IL-18 protect against Burkholderia pseudomallei lung infection while IL-1β is deleterious. PLoS Pathog. 7, e1002452. [PubMed: 22241982]

Chen KW, Groß CJ, Sotomayor FV, Stacey KJ, Tschopp J, Sweet MJ, and Schroder K. (2014). The neutrophil NLRC4 inflammasome selectively promotes IL-1β maturation without pyroptosis during acute Salmonella challenge. Cell Rep. 8, 570–582. [PubMed: 25043180]

Chen KW, Monteleone M, Boucher D, Sollberger G, Ramnath D, Condon ND, von Pein JB, Broz P, Sweet MJ, and Schroder K (2018). Non-canonical inflammasome signaling elicits gasdermin D-dependent neutrophil extracellular traps. Sci. Immunol. 3, eaar6676. [PubMed: 30143554]

Cheng KT, Xiong S, Ye Z, Hong Z, Di A, Tsang KM, Gao X, An S, Mittal M, Vogel SM, et al. (2017). Caspase-11-mediated endothelial pyroptosis underlies endotoxemia-induced lung injury. J. Clin. Invest. 127, 4124–4135. [PubMed: 28990935]

Fernandes-Alnemri T, Wu J, Yu J-W, Datta P, Miller B, Jankowski W, Rosenberg S, Zhang J, and Alnemri ES (2007). The pyroptosome: a supra molecular assembly of ASC dimers mediating inflammatory cell death via caspase-1 activation. Cell Death Differ. 14, 1590–1604. [PubMed: 17599095]

Franchi L, Amer A, Body-Malapel M, Kanneganti T-D, Ozoren N, Jagirdar R, Inohara N, Vandenabeele P, Bertin J, Coyle A, et al. (2006). Cytosolic flagellin requires Ipaf for activation of caspase-1 and interleukin 1beta in salmonella-infected macrophages. Nat. Immunol. 7, 576–582. [PubMed: 16648852]

Hagar JA, Powell DA, Aachoui Y, Ernst RK, and Miao EA (2013). Cytoplasmic LPS activates caspase-11: implications in TLR4-independent endotoxic shock. Science 341, 1250–1253. [PubMed: 24031018]

Hagar JA, Edin ML, Lih FB, Thurlow LR, Koller BH, Cairns BA, Zeldin DC, and Miao EA (2017). Lipopolysaccharide Potentiates Insulin-Driven Hypoglycemic Shock. J. Immunol. 199, 3634–3643. [PubMed: 29038248]

Harly C, Cam M, Kaye J, and Bhandoola A (2018). Development and differentiation of early innate lymphoid progenitors. J. Exp. Med. 215, 249–262. [PubMed: 29183988]

He W-T, Wan H, Hu L, Chen P, Wang X, Huang Z, Yang Z-H, Zhong C-Q., and Han J. (2015). Gasdermin D is an executor of pyroptosis and required for interleukin-1 β secretion. Cell Res. 25, 1285–1298. [PubMed: 26611636]

Jorgensen I, Zhang Y, Krantz BA, and Miao EA (2016). Pyroptosis triggers pore-induced intracellular traps (PITs) that capture bacteria and lead to their clearance by efferocytosis. J. Exp. Med. 213, 2113–2128. [PubMed: 27573815]

Jorgensen I, Rayamajhi M, and Miao EA (2017). Programmed cell death as a defence against infection. Nat. Rev. Immunol. 17, 151–164. [PubMed: 28138137]

Karmakar M, Minns M, Greenberg EN, Diaz-Aponte J, Pestonjamasp K, Johnson JL, Rathkey JK, Abbott DW, Wang K, Shao F, et al. (2020). N-GSDMD trafficking to neutrophil organelles facilitates IL-1β release independently of plasma membrane pores and pyroptosis. Nat. Commun. 11, 2212. [PubMed: 32371889]

Kayagaki N, Warming S, Lamkanff M, Vande Walle L, Louie S, Dong J, Newton K, Qu Y, Liu J, Heldens S, et al. (2011). Non-canonical inflammasome activation targets caspase-11. Nature 479, 117–121. [PubMed: 22002608]

Kayagaki N, Wong MT, Stowe IB, Ramani SR, Gonzalez LC, Akashi-Takamura S, Miyake K, Zhang J, Lee WP, Muszynski A, et al. (2013). Noncanonical inflammasome activation by intracellular LPS independent of TLR4. Science 341, 1246–1249. [PubMed: 23887873]

Kayagaki N, Stowe IB, Lee BL, O'Rourke K, Anderson K, Warming S, Cuellar T, Haley B, Roose-Girma M, Phung QT, et al. (2015). Caspase-11 cleaves gasdermin D for non-canonical inflammasome signalling. Nature 526, 666–671. [PubMed: 26375259]

Kuida K, Lippke JA, Ku G, Harding MW, Livingston DJ, Su MS, and Flavell RA (1995). Altered cytokine export and apoptosis in mice deficient in interleukin-1 beta converting enzyme. Science 267, 2000–2003. [PubMed: 7535475]

Kupz A, Guarda G, Gebhardt T, Sander LE, Short KR, Diavatopoulos DA, Wijburg OLC, Cao H, Waithman JC, Chen W, et al. (2012). NLRC4 inflammasomes in dendritic cells regulate noncognate effector function by memory $CD8^+$ T cells. Nat. Immunol. 13, 162–169. [PubMed: 22231517]

Liu F, and Whitton JL (2005). Cutting edge: re-evaluating the in vivo cytokine responses of $CD8^+$ T cells during primary and secondary viral infections. J. Immunol. 174, 5936–5940. [PubMed: 15879085]

Liu X, Zhang Z, Ruan J, Pan Y, Magupalli VG, Wu H, and Lieberman J (2016). Inflammasome-activated gasdermin D causes pyroptosis by forming membrane pores. Nature 535, 153–158. [PubMed: 27383986]

Maltez VI, and Miao EA (2016). Reassessing the Evolutionary Importance of Inflammasomes. J. Immunol. 196, 956–962. [PubMed: 26802061]

Maltez VI, Tubbs AL, Cook KD, Aachoui Y, Falcone EL, Holland SM, Whitmire JK, and Miao EA (2015). Inflammasomes Coordinate Pyroptosis and Natural Killer Cell Cytotoxicity to Clear Infection by a Ubiquitous Environmental Bacterium. Immunity 43, 987–997. [PubMed: 26572063]

Miao EA, Alpuche-Aranda CM, Dors M, Clark AE, Bader MW, Miller SI, and Aderem A (2006). Cytoplasmic flagellin activates caspase-1 and secretion of interleukin 1beta via Ipaf. Nat. Immunol. 7, 569–575. [PubMed: 16648853]

Miao EA, Leaf IA, Treuting PM, Mao DP, Dors M, Sarkar A, Warren SE, Wewers MD, and Aderem A (2010a). Caspase-1-induced pyroptosis is an innate immune effector mechanism against intracellular bacteria. Nat. Immunol. 11, 1136–1142. [PubMed: 21057511]

Miao EA, Mao DP, Yudkovsky N, Bonneau R, Lorang CG, Warren SE, Leaf IA, and Aderem A (2010b). Innate immune detection of the type III secretion apparatus through the NLRC4 inflammasome. Proc. Natl. Acad. Sci. USA 707, 3076–3080.

Molofsky AB, Byrne BG, Whitfield NN, Madigan CA, Fuse ET, Tateda K, and Swanson MS (2006). Cytosolic recognition of flagellin by mouse macrophages restricts Legionella pneumophila infection. J. Exp. Med. 203, 1093–1104. [PubMed: 16606669]

Ramirez MLG, Poreba M, Snipas SJ, Groborz K, Drag M, and Salvesen GS (2018). Extensive peptide and natural protein substrate screens reveal that mouse caspase-11 has much narrower substrate specificity than caspase-1. J. Biol. Chem. 293, 7058–7067. [PubMed: 29414788]

Rauch I, Deets KA, Ji DX, von Moltke J, Tenthorey JL, Lee AY, Philip NH, Ayres JS, Brodsky IE, Gronert K, and Vance RE (2017). NAIP-NLRC4 Inflammasomes Coordinate Intestinal Epithelial Cell Expulsion with Eicosanoid and IL-18 Release via Activation of Caspase-1 and -8. Immunity 46, 649–659. [PubMed: 28410991]

Rayamajhi M, Zhang Y, and Miao EA (2013). Detection of pyroptosis by measuring released lactate dehydrogenase activity. Methods Mol. Biol. 7040,85–90.

Ren T, Zamboni DS, Roy CR, Dietrich WF, and Vance RE (2006). Flagellin-deficient Legionella mutants evade caspase-1-and Naip5-mediated macrophage immunity. PLoS Pathog. 2, e18–e19. [PubMed: 16552444]

Robinette ML, Bando JK, Song W, Ulland TK, Gilfillan S, and Colonna M (2017). IL-15 sustains IL-7R-independent ILC2 and ILC3 development. Nat. Commun. 8, 14601–14613. [PubMed: 28361874]

Sahillioglu AC, Sumbul F, Ozoren N, and Haliloglu T (2014). Structural and dynamics aspects of ASC speck assembly. Structure 22, 1722–1734. [PubMed: 25458835]

Seyda M, Elkhal A, Quante M, Falk CS, and Tullius SG (2016). T Cells Going Innate. Trends Immunol. 37, 546–556. [PubMed: 27402226]

Shi J, Zhao Y, Wang K, Shi X, Wang Y, Huang H, Zhuang Y, Cai T, Wang F, and Shao F (2015). Cleavage of GSDMD by inflammatory caspases determines pyroptotic cell death. Nature 526, 660–665. [PubMed: 26375003]

Sollberger G, Choidas A, Burn GL, Habenberger P, Di Lucrezia R, Kordes S, Menninger S, Eickhoff J, Nussbaumer P, Klebl, et al. (2018). Gasdermin D plays a vital role in the generation of neutrophil extracellular traps. Sci. Immunol. 3, eaar6689. [PubMed: 30143555]

Tsuchiya K, Nakajima S, Hosojima S, Thi Nguyen D, Hattori T, Manh Le T, Hori O, Mahib MR, Yamaguchi Y, Miura M, et al. (2019). Caspase-1 initiates apoptosis in the absence of gasdermin D. Nat. Commun. 70, 2091.

Wang J, Sahoo M, Lantier L, Warawa J, Cordero H, Deobald K, and Re F (2018). Caspase-11-dependent pyroptosis of lung epithelial cells protects from melioidosis while caspase-1 mediates macrophage pyroptosis and production of IL-18. PLoS Pathog. 74, e1007105–e1007119.

Wang J, Deobald K, and Re F (2019). Gasdermin D Protects from Melioidosis through Pyroptosis and Direct Killing of Bacteria. J. Immunol. 202, 3468–3473. [PubMed: 31036765]

Wiersinga WJ, van der Poll T, White NJ, Day NP, and Peacock SJ (2006). Melioidosis: insights into the pathogenicity of Burkholderia pseudomallei. Nat. Rev. Microbiol. 4, 272–282. [PubMed: 16541135]

Zhao Y, Yang J, Shi J, Gong Y-N, Lu Q, Xu H, Liu L, and Shao F (2011). The NLRC4 inflammasome receptors for bacterial flagellin and type III secretion apparatus. Nature 477, 596–600. [PubMed: 21918512]

Highlights

- NK and T cells produce IFN-γ to prime caspase-11 during *B. thailandensis* infection
- Caspase-1 and caspase-11 cleave gasdermin D in macrophages and neutrophils
- Caspase-11 but not caspase-1 activation leads to pyroptosis in neutrophils
- Neutrophil caspase-11 activation is necessary to clear *B. thailandensis in vivo*

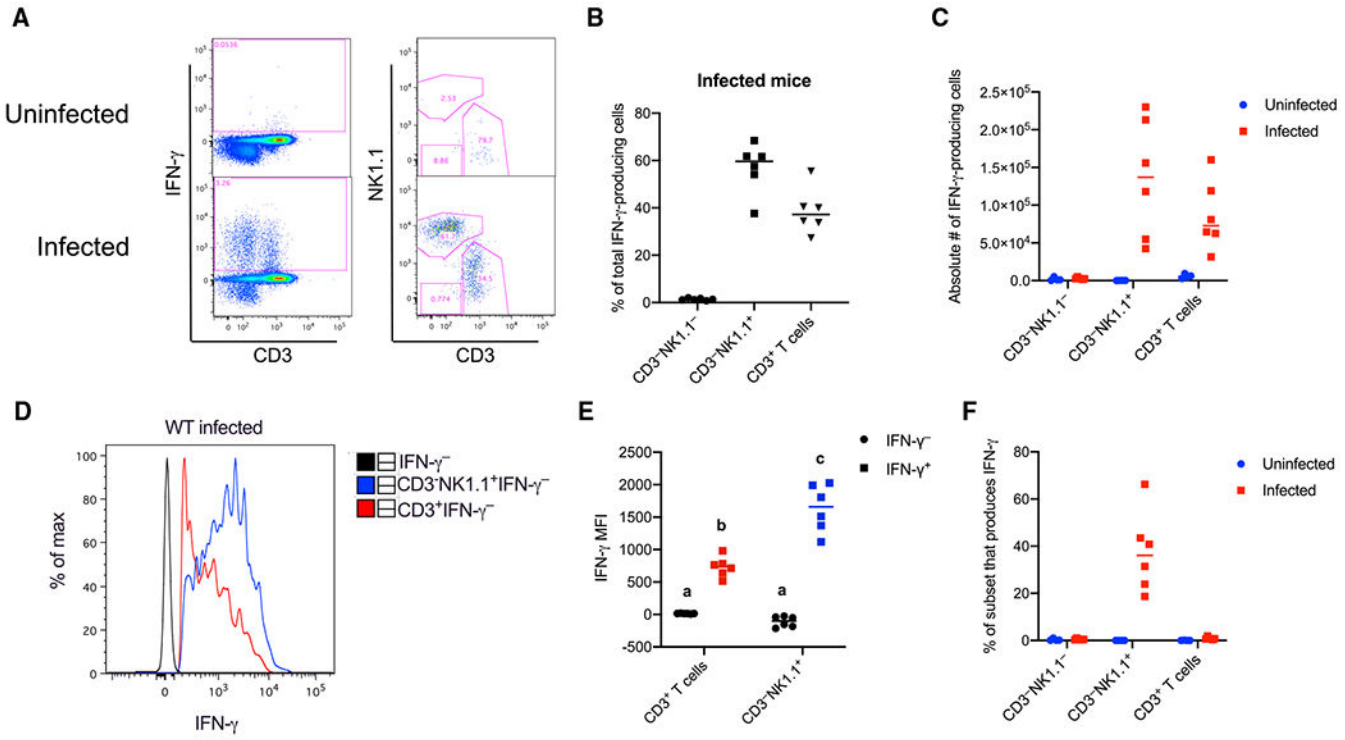

Figure 1. NK Cells and T Cells Are the Primary Producers of IFN-γ during *B. thailandensis* Infection

(A–C) Mice were infected intraperitoneally (i.p.) with 2×10^7 CFU *B. thailandensis*, and 12 h later treated intravenously (i.v.) with 250 mg of brefeldin A. 6 h later, splenocytes were collected (total 18 h post-infection). $Ly6G^-/CD45R^-$ live cells were analyzed by flow cytometry for IFN-γ^+ production. A representative analysis is shown in (A). IFN-γ^+ subpopulations were analyzed for percent of total IFN-γ^+ cells (B) and absolute count (C). (D and E) Geometric mean fluorescent intensity (MFI) of IFN-γ in IFN-γ^+ and IFN-γ^- $NK1.1^+$ and $CD3^+$ subsets were compared by two-way ANOVA. Sidak's multiple comparison test was used for post hoc pairwise comparison between MFI of $NK1.1^+$ and $CD3^+$ subsets from the same sample. Groups that do not share a letter are statistically different from each other with $p \leq 0.05$.

(F) Total spleen populations of $NK1.1^+$ and $CD3^+$ subsets were analyzed for percent that were IFN-γ^+.

All data are pooled from two experiments. Bar represents median.

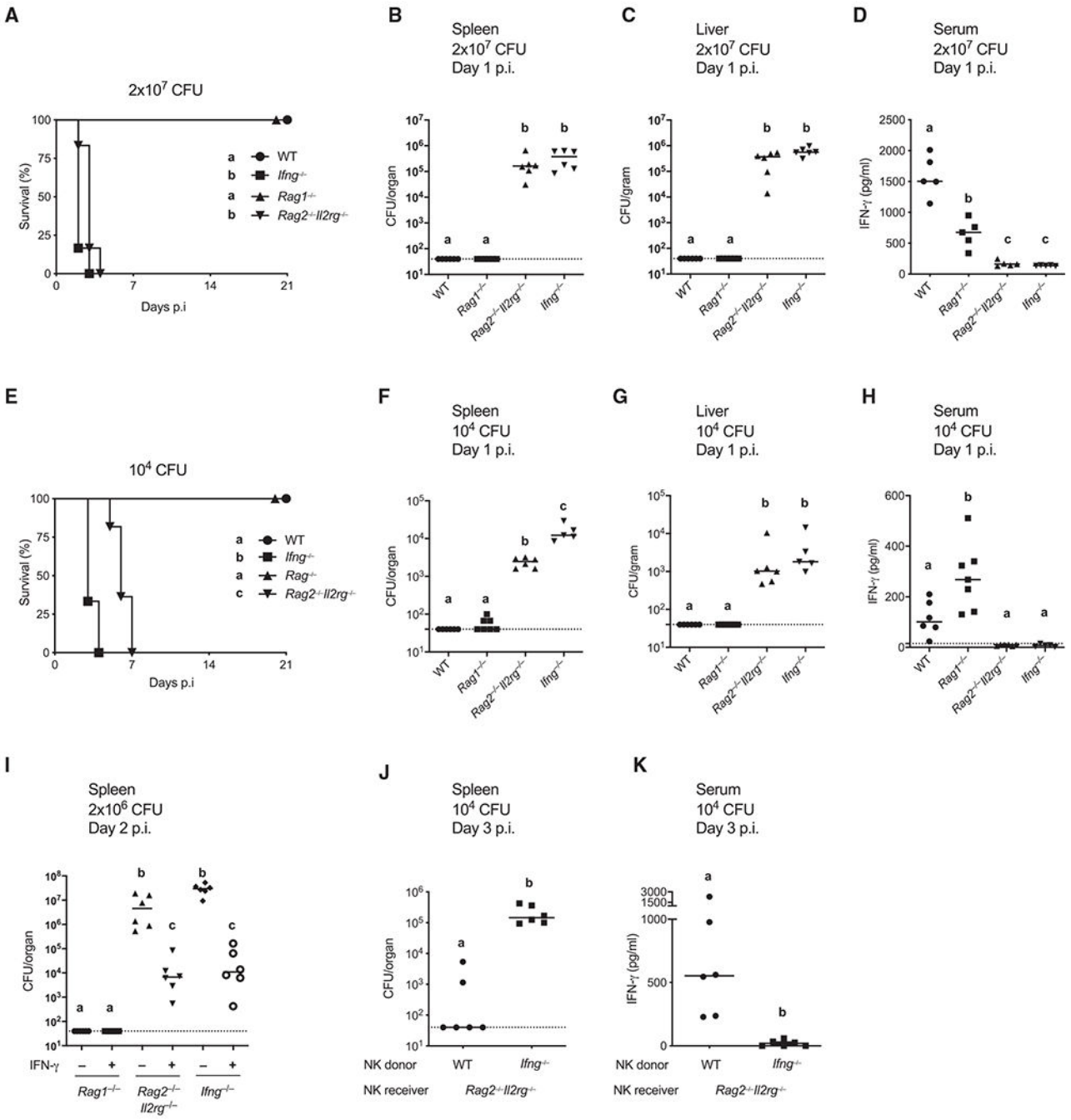

Figure 2. Innate Lymphocyte Production of IFN-γ Is Required for Defense against *B. thailandensis*

(A–H) Mice were infected i.p. with 2×10^7 CFU (A–D) or 104 CFU (E–H) of *B. thailandensis*. Survival was monitored (A and E), or mice were harvested 1 day post infection (p.i.) and bacterial burdens in spleens (B and F) and livers (C and G) were determined, or serum IFN-γ levels were determined by ELISA (D and H).

(I) Mice were infected i.p. with 2×10^6 CFU *B. thailandensis* and injected i.p. with PBS or recombinant mouse IFN-γ (0.5 mg/mouse) at 0 and 24 h p.i. Splenic burdens were determined 48 h p.i.

(J and K) Mice were adoptively treated with 10^6 NK cells at 14 and 7 days prior to infection with 10^4 CFU *B. thailandensis*. Splenic burdens (J) and serum IFN-γ levels, as determined by ELISA (K), were assessed day 3 p.i.

All data are pooled from two experiments. Bar represents median. Dashed line indicates limit of detection. For number of mice in survival panel see Table S1.

Survival curves were compared using log-rank tests using Bonferroni-corrected threshold for statistical significance of $p \leq 0.008$. Bacterial burden and IFN-γ levels were analyzed using one-way ANOVA followed by Tukey's multiple comparisons test with a statistical threshold of $p \leq 0.05$. Groups that do not share a letter are statistically different from each other.

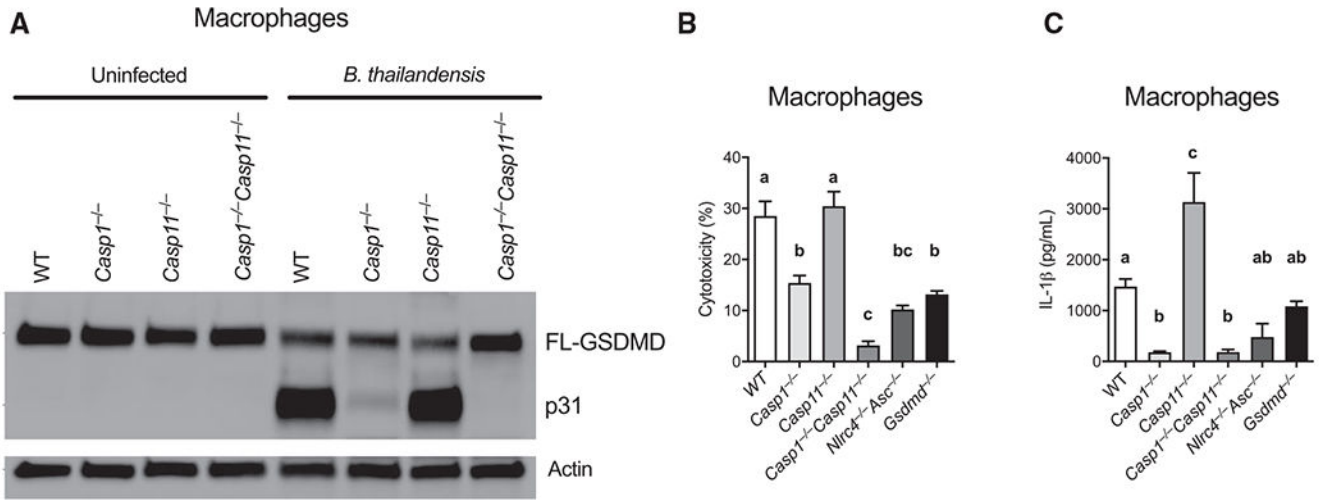

Figure 3. B. thailandensis Induces Gasdermin D-Mediated Pyroptosis and Cytokine Secretion in Macrophages In Vitro

(A–C) Pam_3CSK_4-primed BMMs were infected at MOI 50 for 4 h. Gasdermin D (GSDMD) cleavage was determined by western blot (A), cytotoxicity was determined by LDH release assay (B), and IL-1β was determined by ELISA (C).

Bar represents mean ± SEM. Data are representative of three independent experiments. Data were analyzed using one-way ANOVA followed by Tukey's multiple comparisons test. Groups that do not share a letter are statistically different from each other with $p \leq 0.05$.

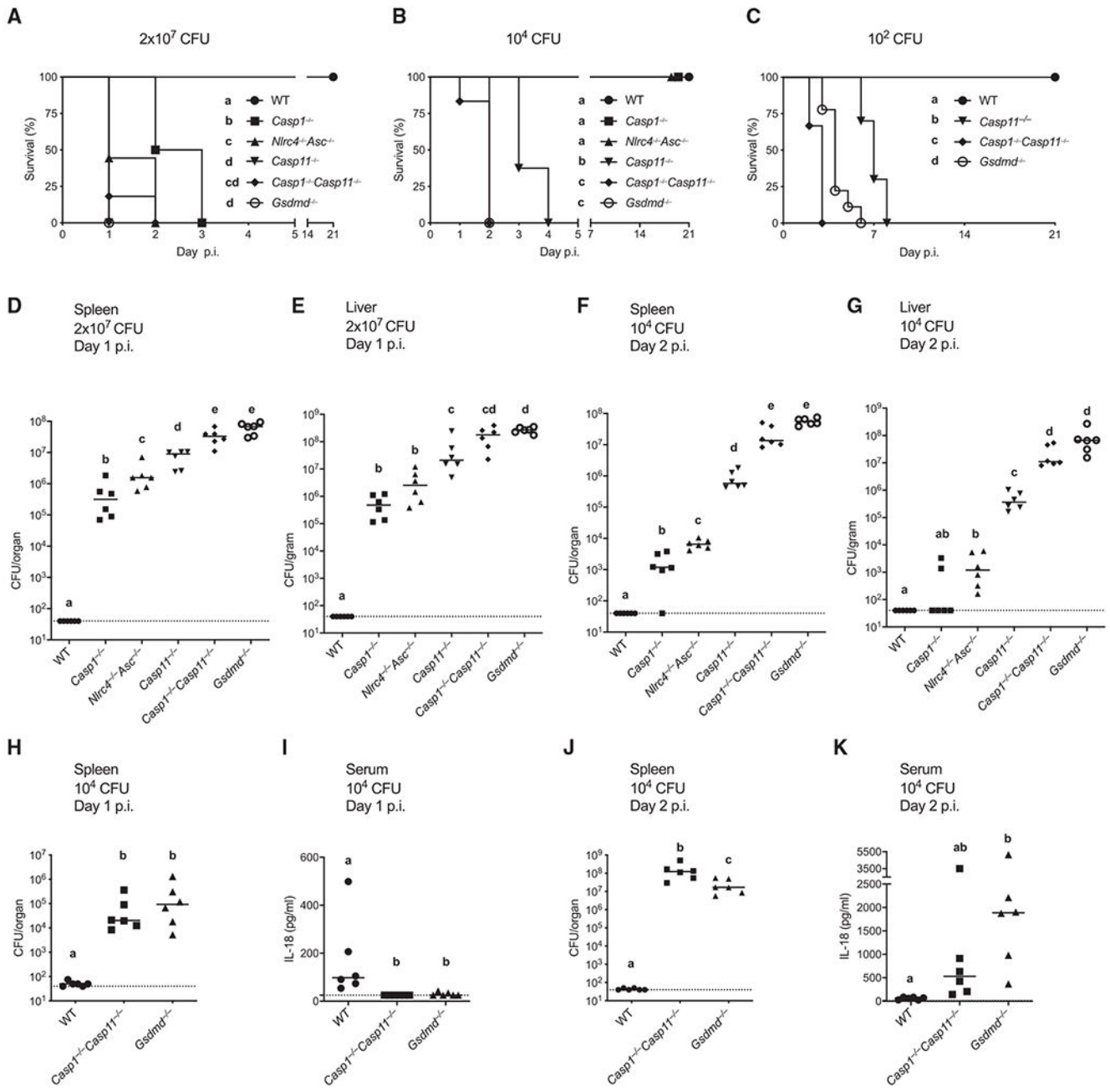

Figure 4. Gasdermin D Is Essential for Defense against *B. thailandensis In Vivo*

(A–C) Mice were infected i.p. with 2×10^7 CFU (A), 10^4 CFU (B), or 10_2 CFU of *B. thailandensis*, and survival was monitored.

(D–G) Mice were infected i.p. with 2×10^7 CFU (D and E) or 10^4 CFU (F and G) of *B. thailandensis,* and bacterial burdens were determined in spleen (D and F) or liver (E and G) at the indicated time post-infection (p.i.).

(H–K) Mice were infected i.p. with 10^4 CFU *B. thailandensis* and bacterial burdens in the spleen were determined on day 1 p.i. (H) or day 2 p.i. (J). Serum IL-18 levels on day 1 p.i. (I) or day 2 p.i. (K) were determined by ELISA.

All data for survival are pooled from three experiments and pooled from two experiments for bacterial burden analysis. Bar represents median. Dashed line indicates limit of detection. For number of mice in survival panel see Table S1. Survival curves were compared using log-rank tests. Bonferroni-corrected thresholds for statistical significance were used ($p \leq 0.003$ for A and B, $p \leq 0.017$ for C). Bacterial burden and IL-18 levels were analyzed using one-way ANOVA followed by Tukey's multiple comparisons test. Groups that do not share a letter are statistically different from each other with $p \leq 0.05$.

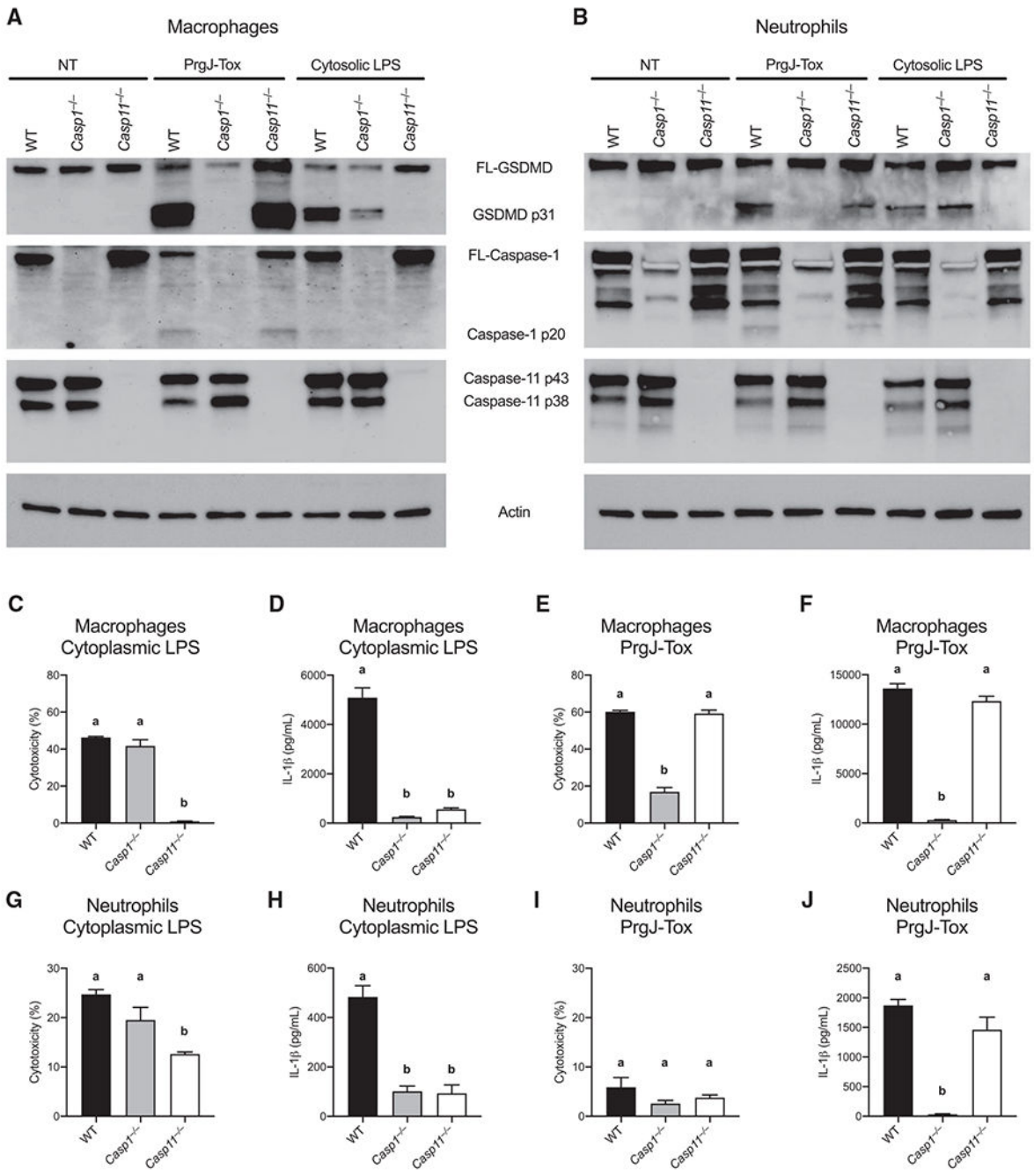

Figure 5. Neutrophils Undergo Pyroptosis in Response to Caspase-11 Agonists but Not NLRC4 Agonists

IFN-γ/LPS-primed macrophages or neutrophils were treated with NLRC4 agonist PrgJ-Tox (2 μg/ml) or transfected by LPS (10 μg/ml) for 5 h. Gasdermin D, caspase-1, and caspase-11 cleavage were determined by western blot in macrophages (A) and neutrophils (B). Cytotoxicity was determined by LDH release assay in macrophages treated with LPS (C) or PrgJ-Tox (E) and neutrophils treated with LPS (G) or PrgJ-Tox (I). IL-1β release was determined by ELISA of supernatant of macrophages treated with LPS (D) or PrgJ-Tox (F) and neutrophils treated with LPS (H) or PrgJ-Tox (J). Bar represents mean ± SEM. Data are

representative of three independent experiments. Cytotoxicity and IL-1β levels were analyzed using one-way ANOVA followed by Tukey's multiple comparisons test. Groups that do not share a letter are statistically different from each other with $p \leq 0.05$. NT, no treatment; FL-GSDMD, full length gasdermin D.

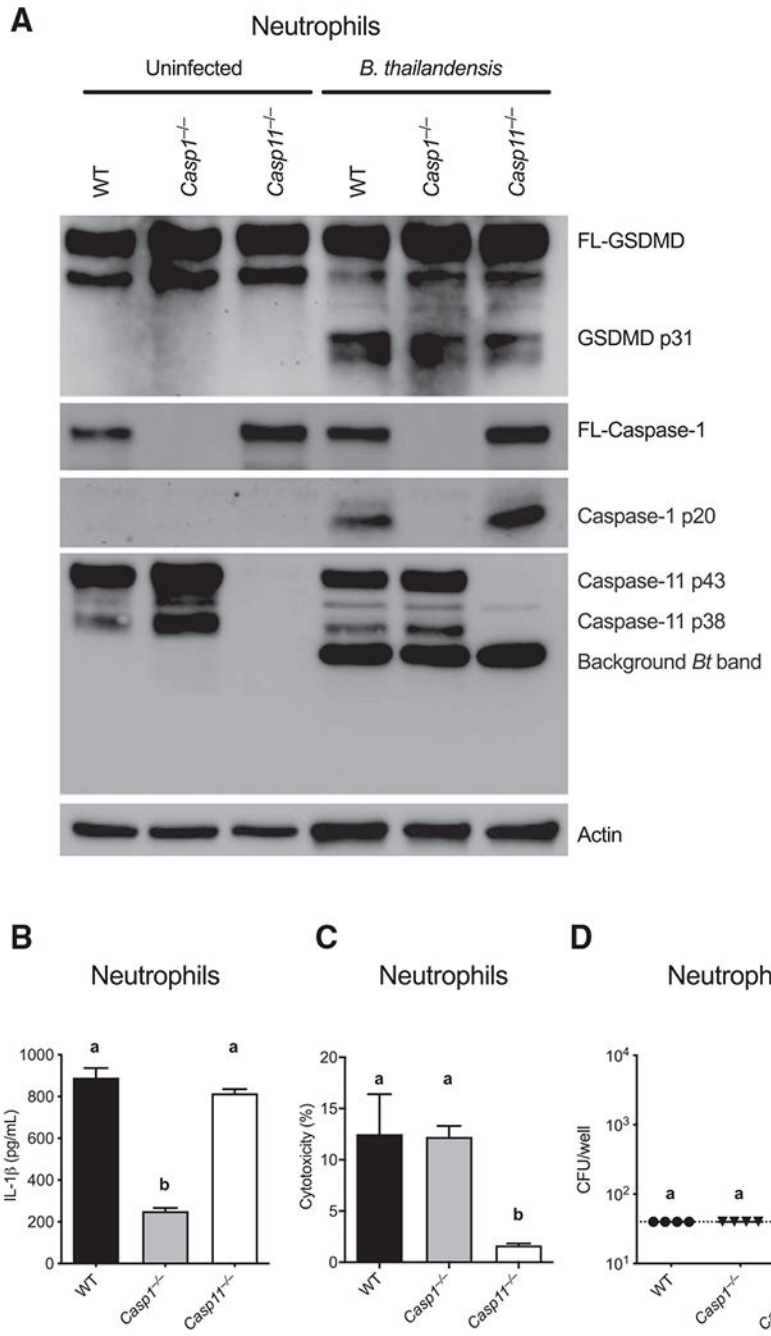

Figure 6. Neutrophils Require Caspase-11 to Trigger Pyroptosis and Clear *B. thailandensis* Infection *In Vitro*

(A–C) Pam_3CSK_4-primed neutrophils were infected with *B. thailandensis* (Bt) at MOI 100 for 5 h. Gasdermin D, caspase-1, and caspase-11 cleavage were determined by western blot (A), IL-1β release was determined by ELISA (B), and cytotoxicity was determined by LDH release assay (C).

(D) Neutrophils were infected at MOI 100 for 4 h. After 1 h, extracellular bacterial growth was stopped by addition of 300 mg/ml kanamycin, and CFU was determined at 4 h. Data are

representative of three independent experiments. Dashed line indicates limit of detection. Bar represents mean ± SEM for (B and C), median for (D).

IL-1β, cytotoxicity, and recovered CFUs were analyzed using one-way ANOVA followed by Tukey's multiple comparisons test. Groups that do not share a letter are statistically different from each other with $p \leq 0.05$. *Bt* background band, background band of *B. thailandensis* components.

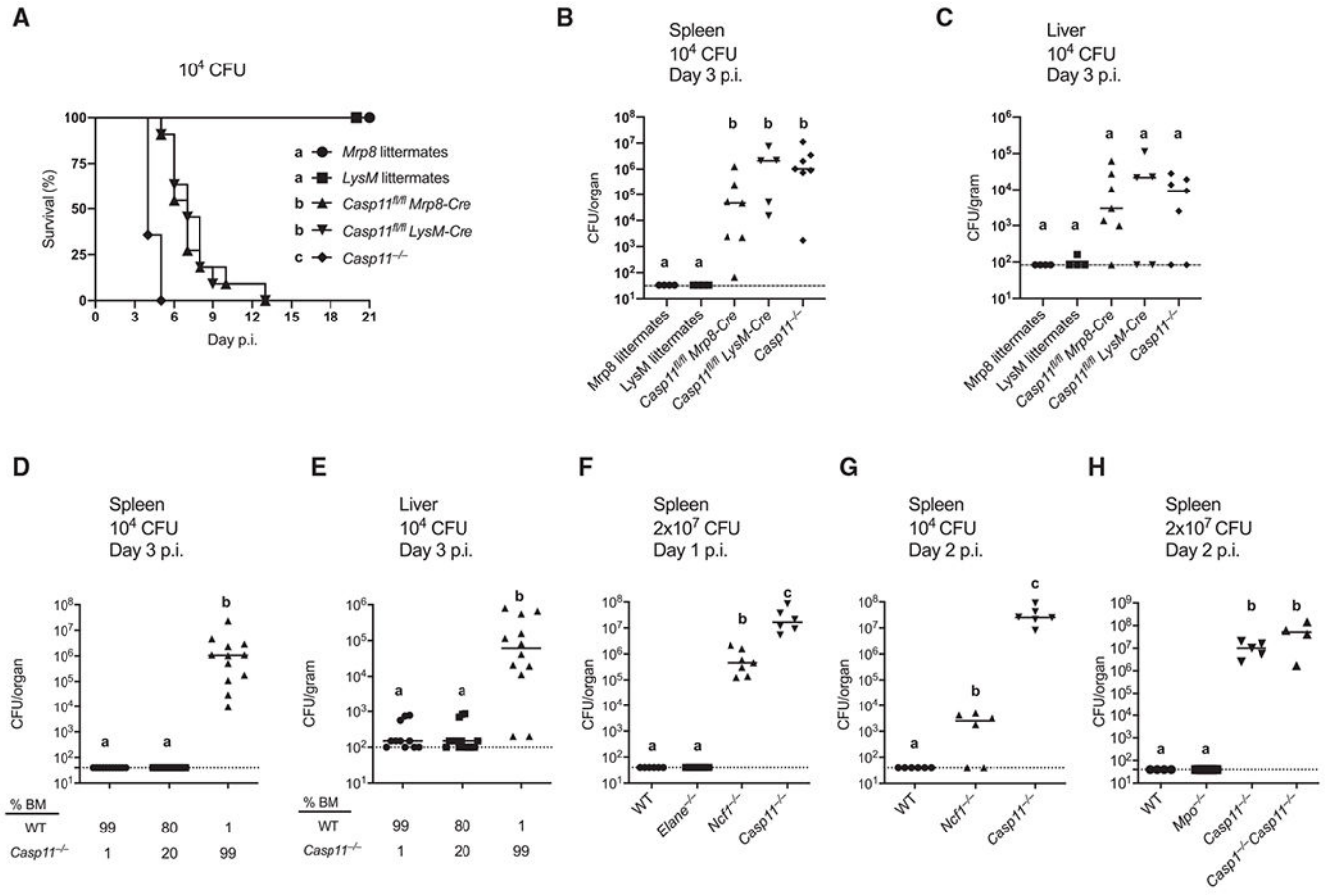

Figure 7. Caspase-11 in Neutrophils Is Essential to Clear *B. thailandensis* Infection *In Vivo*

(A–C) Mice were infected i.p. with 10^4 CFU *B. thailandensis* and survival was monitored (A). Bacterial burdens at 3 days post-infection (p.i.) were determined in spleen (B) and liver (C). *Mrp8* littermate controls and *LysM* littermate controls consisted of *Casp11*$^{+/fl}$ Mrp8-cre and *Casp11*$^{+/+}$ *Mrp8-cre*, and *Casp11*$^{+/fl}$ *LysM-cre* and *Casp11*$^{+/+}$ *LysM-cre*, respectively. (D and E) Lethally irradiated mice were transferred CD45.1$^+$ wild-type and CD45.2$^+$ *Casp11*$^{-/-}$ at the ratios indicated and allowed to engraft for 6 weeks. Mice were then infected i.p. with 10^4 CFU *B. thailandensis*, and splenic (D) and liver (E) bacterial burdens were determined 3 days p.i.(F–H) Mice of the indicated genotypes were infected i.p. with 2 × 10^7 CFU (F and H) or 10^4 CFU (G) of *B. thailandensis*, and splenic burdens were determined either day 1 p.i. (F) or day 2 p.i. (G and H).

All data are pooled from two experiments. Bar represents median. Dashed line indicates limit of detection. For number of mice in survival panel see Table S1. Survival curves were compared using log-rank tests using Bonferroni-corrected threshold for statistical significance of $p \leq 0.005$. Bacterial burdens were analyzed using one-way ANOVA followed by Tukey's multiple comparisons test with a statistical threshold of $p \leq 0.05$. Groups that do not share a letter are statistically different from each other.

KEY RESOURCES TABLE

REAGENT or RESOURCE	SOURCE	IDENTIFIER
Antibodies		
Alexa Fluor (AF) 488 rat anti-mouse CD127 (clone A7R34)	BioLegend	Cat# 135017; RRID: AB_1937206
Brilliant Violet (BV) 570 rat anti-mouse CD3 (clone 17A2)	BioLegend	Cat# 100225; RRID: AB_10900444
APC-Cy7 rat anti-human/mouse CD45R (clone RA3-6B2)	BioLegend	Cat# 103223; RRID: AB_313006
APC-Cy7 rat anti-mouse Ly6G (clone 1A8)	BioLegend	Cat# 127623; RRID: AB_10645331
PE-Cy7 rat anti-mouse CD90.2 (clone 53-2.1)	BioLegend	Cat# 140309; RRID: AB_10645336
BV650 mouse anti-mouse NK1.1 (clone PK136)	BioLegend	Cat# 108735; RRID: AB_11147949
BV421 Armenian hamster anti-mouse TCRgS (clone GL3)	BioLegend	Cat# 118119; RRID: AB_10896753
AF594 rat anti-mouse CD4 (clone GK1.5)	BioLegend	Cat# 100446; RRID: AB_2563182
PE rat anti-mouse CD8 (clone 53-6.7)	BioLegend	Cat# 100708; RRID: AB_312747
APC rat anti-mouse IFN-γ (clone XMG1.2)	BioLegend	Cat# 505810; RRID: AB_315404
Rabbit anti-mouse GSDMD (clone EPR19828)	Abcam	Cat# ab209845; RRID: AB_2783550
Mouse anti-mouse caspase-1 p20 (clone Casper-1)	AdipoGen	Cat# AG-20B-0042-C100; RRID: AB_2755041
Rabbit anti-mouse caspase-11 (clone EPR18628)	Abcam	Cat# ab180673
Mouse anti-actin (clone ACTN05 (C4))	Thermo Fisher Scientific	Cat# MA5-11869; RRID: AB_11004139
Bacterial and Virus Strains		
Burkholderia thailandensis, strain E264-1, passaged through *Casp1*$^{-/-}$*Casp11*$^{-/-}$ mice	Aachoui et al., 2015	N/A
Chemicals, Peptides, and Recombinant Proteins		
LIVE/DEAD Fixable Blue Dead Cell Stain Kit	ThermoFIsher Scientific	Cat# L23105
Pam_3CSK_4	InvivoGen	Cat# tlrl-pms
Recombinant mouse IFN-γ	Peprotech	Cat# 315-05
Ultrapure LPS, *E. coli* O111:B4	Invivogen	Cat# tlrl-3pelps
PrgJ-Tox	Zhao et al., 2011	N/A
Critical Commercial Assays		
Mouse IL-1 beta/IL-1 F2 DuoSet ELISA	R&D Systems	Cat# DY401
Mouse IL-18 ELISA Kit	MBL International	Cat# 7625
Neutrophil Isolation Kit, mouse	Miltenyi Biotec	Cat# 130-097-658
Deposited Data		
IL18R1, IL18RAP expression data	The Immunological Genome Project (http://rstats.immgen.org/Skyline_microarray/skyline.html)	Microarray database. IL18R1 (probe set ID 10345807); IL18RAP (probe set ID 10345824)
Experimental Models: Organisms/Strains		

REAGENT or RESOURCE	SOURCE	IDENTIFIER
Mouse: Wild type (WT): C57BL/6J	The Jackson Laboratory	JAX# 000664
Mouse: *Ifng*$^{-/-}$; B6.129S7-*Ifng*^{tm1Ts}/J	The Jackson Laboratory	JAX# 002287
Mouse: *Rag1*$^{-/-}$; B6.129S7-*Rag1*^{tm1Mom}/J	The Jackson Laboratory	JAX# 002216
Mouse: *Rag2*$^{-/-}$*Il2rg*$^{-/-}$: C57BL/6NTac;B10(Cg)-*Rag2*^{tm1Fwa}*Il2rg*^{tm1Wjl}	Taconic	Taconic# 4111
Mouse: Nlrc4$^{-/-}$Asc$^{-/-}$: C57BL/6N	Aachoui et al., 2015	N/A
Mouse: *Casp1*$^{-/-}$: C57BL/6N	Rauch et al., 2017	N/A
Mouse: *Casp11*$^{-/-}$: C57BL/6N	Kayagaki et al., 2011	N/A
Mouse: *Casp1*$^{-/-}$*Casp11*$^{129mut/129mut}$ referred to as *Casp1*$^{-/-}$*Casp11*$^{-/-}$	Kuida et al., 1995	N/A
Mouse: *Gsdmd*$^{-/-}$: C57BL/6	Rauch et al., 2017	N/A
Mouse: *Casp11*$^{fl/fl}$: C47BL/6	Cheng et al., 2017	N/A
Mouse: *LysM-cre*: B6.129P2-*Lyz2*$^{tm1(cra)Ifo}$/J	The Jackson Laboratory	JAX# 004781
Mouse: *Mrp8-cre*: B6.Cg-Tg(S100A8-cre,-EGFP)1Ilw/J	The Jackson Laboratory	JAX# 021614
Mouse: *Elane*$^{-/-}$: B6.129X1-*Elane*^{tm1Sds}/J	The Jackson Laboratory	JAX# 006112
Mouse: *Mpo*$^{-/-}$: B6.129X1-*Mpo*^{tm1Lus}/J	The Jackson Laboratory	JAX# 004265
Mouse: *Ncf1*$^{mt/mt}$ referred to as *Ncf1*$^{-/-}$: B6(Cg)-*Ncf1*^{m1J}/J	The Jackson Laboratory	JAX# 004742
Mouse: *Prf1*$^{-/-}$: C57BL/6-*Prf1*^{tm1Sdz}/J	The Jackson Laboratory	JAX# 002407
Software and Algorithms		
Prism 8	GraphPad	N/A
FlowJo version 9.9.6	TreeStar	N/A